

To determine the effect of thermal shock  
On a fixed glass dome



Author

Shafique-ur-rehman

Regn Number

00000276239

Supervisor

Dr.Mushtaq Khan

DEPARTMENT OF DESIGN AND MUFACTURING ENGINEERING  
SCHOOL OF MECHANICAL & MANUFACTURING ENGINEERING  
NATIONAL UNIVERSITY OF SCIENCES AND TECHNOLOGY  
ISLAMABAD  
October, 2020

To determine the effect of thermal shock on a  
fixed glass dome

Author

Shafique-ur-rehman

Regn Number

00000276239

A thesis submitted in partial fulfillment of the requirements for the degree of  
MS Design and Manufacturing Engineering

Thesis Supervisor:

Dr.Mushtaq Khan

Thesis Supervisor's Signature: \_\_\_\_\_

DEPARTMENT OF DESIGN AND MUFACTURING ENGINEERING  
SCHOOL OF MECHANICAL & MANUFACTURING ENGINEERING  
NATIONAL UNIVERSITY OF SCIENCES AND TECHNOLOGY,

ISLAMABAD

October , 2020

## **THESIS ACCEPTANCE CERTIFICATE**

Certified that final copy of MS/MPhil thesis Written by Mr. Shafique-ur-rehman (Registration No: 00000276239), of SMME (School of Mechanical and Manufacturing Engineering) has been vetted by undersigned, found complete in all respects as per NUST Statutes/ Regulations, is free of plagiarism, errors and mistakes and is accepted as partial fulfillment for award of MS/MPhil Degree. It is further certified that necessary amendments as pointed out by GEC members have also been incorporated in this dissertation.

Signature: \_\_\_\_\_

Name of the supervisor: Dr. Mushtaq Khan

Dated: \_\_\_\_\_

Signature (HOD): \_\_\_\_\_

Dated: \_\_\_\_\_

Signature (Principal): \_\_\_\_\_

Dated: \_\_\_\_\_

## **MASTER THESIS WORK**

We hereby recommend that the dissertation prepared under our supervision by: Shafique-ur-rehman 00000276239 Titled: “to determine the effects of thermal shock on a fixed glass dome” be accepted in partial fulfillment of the requirements for the award of MS Design and Manufacturing Engineering degree with (.....) grade.

### **Examination Committee Members**

1. Name: Dr.Hussain Imran Signature: \_\_\_\_\_

2. Name: Dr.Emad ud Din Signature: \_\_\_\_\_

3. Name: Dr.Najmul Qadir Signature: \_\_\_\_\_

Supervisor's name: Dr.Mushtaq Khan Signature: \_\_\_\_\_

Date: \_\_\_\_\_

\_\_\_\_\_  
Head of Department

Date: \_\_\_\_\_

### **COUNTERSIGNED**

\_\_\_\_\_  
Dean/principal

Date: \_\_\_\_\_

## **Declaration**

It is certify that this research work titled “to determine the effects of thermal shock on a fixed glass dome” is my own work. The work has not been presented elsewhere for assessment. The material that has been used from other sources. It has been properly acknowledged / referred.

Signature of Student

Shafique-ur-rehman

2018-NUST-MS-DME-00000276239

## **Plagiarism certificate (Turnitin Report)**

This thesis has been checked for Plagiarism. Turnitin report endorsed by Supervisor is attached.

Signature of Student

Shafique-ur-rehman

2018-NUST-MS-DME-00000276239

Signature of the supervisor

## **Copyright statement**

- Copyright in text of this thesis rests with the student author. Copies (by any process) either in full, or of extracts, may be made only in accordance with instructions given by the author and lodged in the Library of NUST School of Mechanical & Manufacturing Engineering (SMME). Details may be obtained by the Librarian. This page must form part of any such copies made. Further copies (by any process) may not be made without the permission (in writing) of the author.
- The ownership of any intellectual property rights which may be described in this thesis is vested in NUST School of Mechanical & Manufacturing Engineering, subject to any prior agreement to the contrary, and may not be made available for use by third parties without the written permission of the SMME, which will prescribe the terms and conditions of any such agreement.
- Further information on the conditions under which disclosures and exploitation may take place is available from the Library of NUST School of Mechanical & Manufacturing Engineering, Islamabad

## **Acknowledgement**

I am thankful to my Creator Allah Subhana-Watala to have guided me throughout this work at every step and for every new thought which you setup in my mind to improve it. Indeed I could have done nothing without your priceless help and guidance. Whosoever helped me throughout the course of my thesis, whether my parents or any other individual was your will, so indeed none be worthy of praise but you.

I am profusely thankful to my beloved parents who raised me when I was not capable of walking and continued to support me throughout in every department of my life. Especially my father who is the real boss of my life. He has planned my life quite efficiently and teaches me to do hard work whatever the circumstances are.

I would also like to express special thanks to my supervisor Dr.Mushtaq khan for his help throughout my thesis and also for the motivation and determination he gave me. He cares so much about any of his student's work and responds to queries and question so promptly.

I would also like to pay special thanks to Dr.Emad ud din for his tremendous support and cooperation. Each time I got stuck in something, he came up with the solution. Without his help I wouldn't have been able to complete my thesis. I appreciate his patience and guidance throughout the whole thesis.

I would also like to thank Mr.kashif Masood , Dr.Mujahid badshah and Mr.Usmaan aslam for being on my thesis guidance.

Finally, I would like to express my gratitude to all the individuals who have rendered valuable assistance to my study.



*Dedicated to my exceptional parents and adored siblings whose tremendous support and cooperation led me to this wonderful accomplishment.*

## **Abstract**

An infrared (IR) homing of an aircraft is an enclosure that protects the infrared (IR) seeker, enhances the aerodynamic ability of the dome and decreases the resistance in flying. It also protects IR seeker which is important for cueing of targets and tracking of the final approach. High speed aircrafts mostly consist of glass domes in the front that are clamped or bonded inside a metallic housing. A sudden short duration of high speed during a chase is encountered in which the bonded dome has to bear the pressure and a frictional rise in temperature on the outer surface whereas the inner surface will not be able to reach the same temperature. This sudden rise in temperature and the resultant uneven temperature distribution on the outer and inner surface along with the air pressure creates stresses in the dome mostly due to thermal shock and difference in coefficients of thermal expansions of the metal and glass. Thus, the material of the dome must have good mechanical properties to withstand thermal shock. In this thesis, a thermal-structural coupled analysis of the dome has been performed based on two materials i-e BK7 and spinel. The temperature and pressure loads derived from the fluent have been forced on to the surface of the dome which yields maximum stress ( $\sigma$ ), maximum deformation and thermal shock on the dome. The results are analyzed to find the Survivability of the dome

**Keywords:** thermal shock, dome, maximum stress

## Table of Contents

<b>Declaration.....</b>	<b>v</b>
<b>Plagiarism certificate (Turnitin Report).....</b>	<b>vi</b>
<b>Copyright statement .....</b>	<b>vii</b>
<b>Acknowledgement .....</b>	<b>viii</b>
<b>Abstract.....</b>	<b>1</b>
<b>Chapter 1 Introduction.....</b>	<b>6</b>
1.1 Overview.....	6
1.2 Project phasing:.....	7
<b>Chapter 2 : Literature review .....</b>	<b>9</b>
<b>Chapter 3 Benchmarking .....</b>	<b>12</b>
3.1 Modeling and analysis .....	12
3.2 Results and discussions:.....	13
3.3 A Summary: .....	14
<b>Chapter 4 Design &amp; Development Methodology .....</b>	<b>15</b>
4.1 Problem Statement .....	15
4.2 Flow requirements: .....	15
4.3 Ansys/Fluent .....	16
4.3.1 Geometric Modelling: .....	16
4.3.2 Computational domain:.....	16
4.3.3 Steady and transient analysis with heat transfer: .....	18
4.3.4 Non-uniform flow .....	19
4.3.5 Numerical approach: .....	20
4.3.6 Discussion: .....	22
4.3.7 Results:.....	22
4.4 Materials: .....	23

4.5	Thermal-structural analysis:.....	25
4.5.1	Geometry: .....	25
4.5.2	Model and setup:.....	25
4.5.3	Meshing: .....	25
4.5.4	Transient thermal: .....	26
4.5.5	Thermal-structural coupling:.....	26
4.5.6	Discussion: .....	26
<b>Chapter 5</b>	<b>:Conclusion and future work .....</b>	<b>35</b>
5.1	Conclusion .....	35
5.2	Future work.....	37
<b>References</b> .....		<b>38</b>

## List of Figures

<b>Figure 1:</b> Thermal shock effect on IR optical dome .....	6
<b>Figure 2:</b> Meshing comparison .....	12
<b>Figure 3:</b> static pressure at Mac=2 .....	13
<b>Figure 4:</b> static pressure at Mac=2.5 .....	14
<b>Figure 5:</b> static pressure at Mac=3 .....	14
<b>Figure 6:</b> CAD model .....	16
<b>Figure 7:</b> computational domain .....	17
<b>Figure 8:</b> boundary layer.....	17
<b>Figure 9:</b> Grid Independency .....	18
<b>Figure 10:</b> static pressure contours at Mac=4.5 .....	18
<b>Figure 11:</b> static temperature at Mac=4.5 .....	19
<b>Figure 12:</b> input profile for Case I .....	19
<b>Figure 13:</b> Input profile for case II.....	20
<b>Figure 14:</b> static temperature profile at the dome surface.....	22
<b>Figure 15:</b> static pressure profile at the dome surface .....	23
<b>Figure 16:</b> properties of BK7 .....	24
<b>Figure 17:</b> properties of spinel .....	25
<b>Figure 18:</b> Meshing of the model.....	25
<b>Figure 19:</b> Maximum principal stresses in BK7 dome (case I).....	27
<b>Figure 20:</b> deformation in BK7 dome (case I) .....	27
<b>Figure 21:</b> Maximum principal stress in spinel dome (case I).....	28
<b>Figure 22:</b> deformation at spinel dome (case I) .....	28
<b>Figure 23:</b> Maximum principal stresses in BK7 dome(case II) .....	29
<b>Figure 24:</b> deformation in BK7 dome (case II).....	29
<b>Figure 25:</b> Maximum principal stresses in spinel dome (case II) .....	30
<b>Figure 26:</b> deformation in spinel dome (case II).....	30
<b>Figure 27:</b> Temepature difference at the surface of BK7 dome (case I).....	31
<b>Figure 28:</b> Temperature difference at the surface of the spinel dome (case I).....	31
<b>Figure 29:</b> Temperature difference at the surface of the BK7 dome (case II).....	32
<b>Figure 30:</b> Temperature difference at the surface of the spinel dome (case II) .....	32
<b>Figure 31:</b> Heat flux at the BK7 dome (case I) .....	33
<b>Figure 32:</b> Heat flux at spinel dome (case I).....	33

<b>Figure 33:</b> Heat flux at BK7 dome (case II) .....	34
<b>Figure 34:</b> Heat flux at spinel dome (case II).....	34
<b>Figure 35:</b> Maximum principal stresses profile for BK7 and spinel (case I) .....	35
<b>Figure 36:</b> Maximum principal stresses profile for BK7 and spinel (case II).....	36

## List of Tables

<b>Table 1:</b> A comparison .....	14
<b>Table 2:</b> input boundary conditions.....	21
<b>Table 3:</b> FS calculated for all the cases .....	37

# Chapter 1 Introduction

## 1.1 Overview

The development and application of infrared optical and infrared technology has a higher requirements in material science because equipment of new generation like infrared viewer, thermal infrared imager, infrared-guided aircrafts etc. work at severe conditions. Many advanced air defense systems have developed infrared (IR) seeker to maintain the right direction and focus of high speed aircrafts on their targets. These high speed aircraft create a severe aerothermal environment that must be resist by the windows known as IR dome. Researchers have proposed number of different shape domes which includes conical, ellipsoid, on Kamran, tangent ogive etc. Below Mach 0.8, the pressure drag at the dome is essentially zero for all shapes and the pressure drag increases exponentially in the transonic region and beyond where the effects of the pressure drag becomes high. Similarly pressure drags is maximum for blunt bodies and minimum for the parabola shapes. Most of the time, tangent ogive shapes are preferred to with stand the aerodynamic drag. The high heat fluxes during flight induces an abrupt temperature gradients that causes thermal shock failure of the dome. Thermal shock failure of the dome during the experiment has been shown in figure 1.

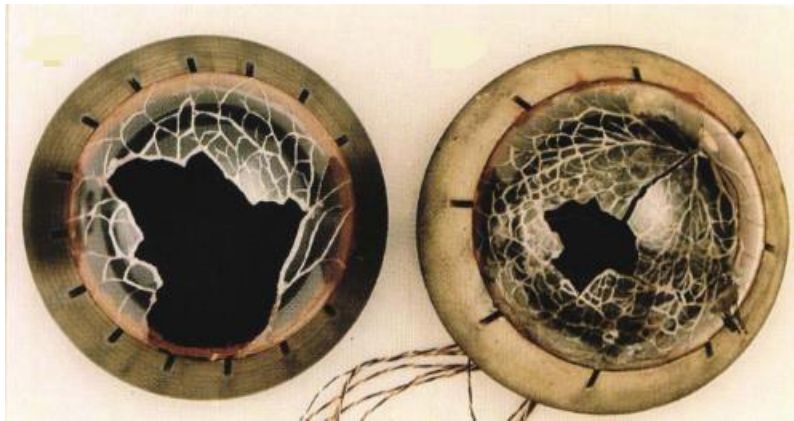


**Figure 1:** Thermal shock effect on IR optical dome

The two important parameters that are important in withstanding the thermal shock failure are dome material and dome attachment. A material with good mechanical, chemical and physical properties is the most suitable for IR dome. Researchers have worked on the dome materials to get the highly durable and efficient materials with good performance. Experimentally, Number of materials have been tested to find out their ability to meet supersonic flight requirements which includes germania glass, zinc sulfide, lanthana, spinel etc. These IR optical domes have also been tested by varying the

wall thickness i-e from 0.055 in to 0.1 in. Other factors which play an important role in survivability of the dome are bonding material and housing of the dome. The formation of cracks in the adhesive cause it to break and paves the way for the generation of thermal shock failure. That's why, difference in the coefficient of thermal expansion between dome and adhesive is inversely proportional to its performance. Moreover, housing of the dome has its own importance which holds the dome via adhesive. Similarly, the dome attachment has been given a considerable importance in the past. The primary objective of the dome attachment is to resist the penetration of thermal stresses into the dome. Several numerical models have also been developed to predict the thermal response of the IR seeker windows against the supersonic flight. Mac number ranging from 1 to 6 have been simulated using simulation software.

This project is composed of several steps. Designing of the CAD model is the first step of the numerical study. The developed CAD model is then transferred to meshing section where multiple meshes i-e coarse, medium and fine, are applied to the CAD model. These meshes are solved using the relevant models to find out the optimized mesh. This process is called mesh independency study. The next phase is to apply the boundary conditions on the optimized mesh model and select the most appropriate model to solve the system of equations which yields the results. The numerical results have been validated by the experimental data which is taken using temperature and stain gauges. This methodology has been used in the design and production of IR seeker system.

Objectives:

My research work includes

- To benchmark a research paper as a model paper
- To develop a finite element (FE) model
- To analyze the effect of temperature variation over the dome and metal housing at high speeds
- To analyze the residual stresses on dome and metal housing at high speed.

## **1.2 Project phasing:**

Ansys has been used to find out the variation of temperature and pressure over the dome w.r.t time which leads to the thermal shock failure. The project has five phases.



Project starts from design modular where a CAD model of the dome along with adhesive and housing is modeled. The CAD model is transferred to ICEM CFD tool where an optimized mesh is generated. The meshed model is exported to fluent where aerodynamic analysis for two cases i-e mac 2.5 and mac 3.5 is done. A variable flow, from 0-2.5 and 0-3.5 mac in 20 and 25 seconds respectively, is passed over the surface of the dome which yields temperature and pressure variation over the dome. The temperature and pressure variation over the dome is forced on to the surface of the dome. Next step is to perform a thermal-structural coupled analysis of the dome which yields the maximum stress, maximum deformation and temperature difference on the inner and outer surface of the dome. These parameters are manipulated to find out the thermal shock failure of the dome.

## Chapter 2 : Literature review

IR optical domes are extensively employed in high speed aircrafts. To meet the requirement of IR domes, materials of dome must have the combination of excellent optical, mechanical and chemical properties. Various researcher have published the numerical studies and experimental work related to IR domes in some prestigious journals. Limits to design of an IR dome is proposed by You tang Gao [1]. They explained the thermal shock phenomenon according to the aerodynamic theory and thermal shock theory. They proposed that windows of the optical parts has a curvature radius which is a function of the pressure difference. This difference in pressure can cause aberration changes. The brittle fracture of the material will be caused if the maximum stresses goes beyond the strength which is permitted for the material. They assumed an ideal material for IR dome that should have high strength, high thermal conduction coefficient, low thermal radiation, low thermal expansion, erosion to wind sand and water, radiation resistance of ultrasonic. They concluded that no material can meet the above requirements completely. The phenomenon of cracks propagation in the transparent materials due to thermal shocks has also been explained by researchers [2]. They simulated the response of the thermal stresses using finite element method. The Mohr coulomb criterion was employed to predict the initiation. They concluded that the maximum stress is located at the edge of the glass pane between the hot and cool glass parts and the stress fluctuates seriously at later stage before crack initiation. Under a slow rate of temperature rise, the thermal stress are very small and can be minimized while under a fast rate of temperature rise, a small temperature can rise create the thermal stresses which neither be ignored nor controlled. A cooling system is also proposed to reduce the aerodynamic affects and it was found that not only the aero-optical disturbances becomes negligible but shock waves were also reduced [3]. Jiang Zhenhai and Ai Xingjian performed thermal-structural analysis of supersonic dome based on three materials i-e MgF<sub>2</sub>, Al<sub>2</sub>O<sub>3</sub> and ZnS [4]. They performed an aerodynamic analysis on an IR dome using k-omega model and extracted the maximum temperature and maximum pressure acting on the surface of the dome. In the second step, they transferred the thermal and pressure loads from fluent to static thermal and static structural respectively. A flow of Mac 2.5 was passed over the dome. Maximum pressure of 8MPa and maximum temperature of 695K were applied to three domes with different materials. They found Al<sub>2</sub>O<sub>3</sub> as the most suitable material for a supersonic dome. Similarly, Denish Davis and Francis Mathew made a design and performed an analysis on different types of aircraft radomes [5].

They simulated three radomes with different material properties .They proved that high speed radomes are found to be the best one. Sebastian Marian Zaharia also performed a CFD simulation and FEA simulation on an infrared homing to find out the areas where stress and deformations are maximum [6].He proposed a new design to minimize the stresses and structure rigidity .The flight carried out in a range of 20-80 km reaching a speed of Mac 7.He observed that the skin made up of double skin of titanium yields a good resistance to elastic deformation. At the same time, aircraft cannot fly at the same speed when angle of attack is changing but fluctuates around Mac 6.5. A similar analysis is performed by M. Sreenivasula reddy and N. Keerthi [7].They proposed a new nose concept over existing conventional nose designs. Two models were proposed with different nose radius and materials i-e Titanium Ti-6Al-4V and Titanium Ti-6Al-6V-2SN.They proved that Titanium Ti-6Al-4V is the suitable material for nose with less deformation and von-Moises stress. A similar analysis is performed by Jinsong Huang on a composite dome under axial load and internal pressure [8].He developed a model to calculate stability of the dome under axial compression and external pressure. He concluded that stress distribution over a structure originates from a high stress zone and fluctuates towards the ends. Structure fails when the maximum stress reaches a critical stress point .However, the structure still has some bearing capacity for high loading. Bin Tang and Yi Yang investigated the crystallization mechanism of Barium Gallogermanate Glass [9].They proposed the germinate glass as a potential candidate material for IR domes and windows. Charles T. Warner tested ALON for its various mechanical and optical properties and found it as the best material for severe environment [10]. ALON is considered superior to sapphire for the thermal shock failure. Due to its low cost and fabrication, it will continue to replace sapphire. Great interest is also been shown on heat flux data gained from ISL shock tunnel experiments [11]. These were done for Mach number between 3.5 and 10 for flight altitude conditions ranging from sea level up to 60 km. The obtained results are compared with calculations based on the classical boundary layer theory for the turbulent as well as for the laminar boundary layer formation at a conical aircraft nose. Best agreement exists between the heat fluxes measured and the analytical solutions for a sharp cone. Number of other experiments have been done on ISL shock tunnel experiment to find out the heating at the tip of the hypersonic IR homing. J. srulijes and f. seiler performed a similar experiment to find the heat flux at the tip of the dome [12]. The heat flux measurements performed at a flight altitude of 15 km show a laminar to turbulent boundary layer transition while the boundary layer at a flight altitude of 21 km develops fully laminar. Claude A. Klein provides formulas and the explained the

complete process of the thermal shock in a body [13]. He states that the attachment of the dome with the body plays important part in weakness of the dome. He also introduced the Biot number as a function of the thermal shock. In a thermally thin regime ( $Bi < 1$ ), the thickness of the window or dome plays a critical role in the sense that minimizing the thickness enhances the ability to withstand thermal shocks.

## Chapter 3 Benchmarking

In the first phase of the project, three cases from a journal paper have been solved as a Benchmark [14]. The study of the aerodynamic performance of the aircraft which operates in supersonic Flows has been carried out. The aerodynamics of the object within supersonic flows varies which is necessary to understand when working on efficient design. The paper analyzes the effects of spikes on the characteristics and performance of the body. However, three models from the paper have been solved and verified as a benchmark.

### 3.1 Modeling and analysis

2D models were developed for each case and analyzed for the required conditions in Fluent. Since the model is considered as Axisymmetric, a 2D model has been considered instead of completed 3D model to reduce the computational cost and get a comparatively better results by eliminating 3D meshing errors. Meshing is done in ICEM CFD tool. In this meshing method, the domain is meshed fine around the body to capture the shock waves. The mesh generated is given below:

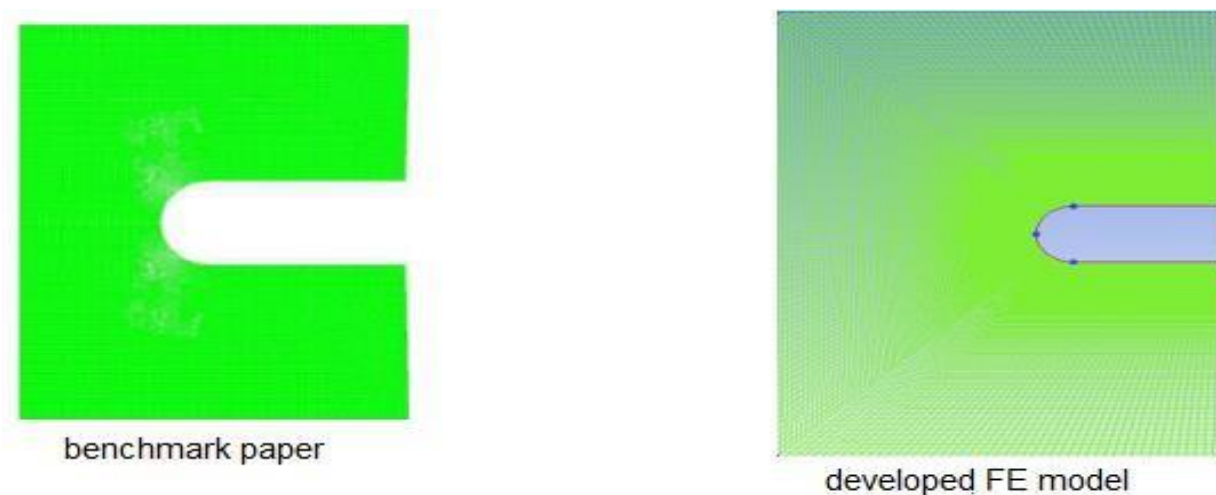


**Figure 2:** Meshing comparison

Density based solver is utilized to solve the problem. In the viscous models, k-omega SST model is selected because of its good performance against turbulent flows. As this problem contains far field, ideal gas is selected from the density box. The boundary conditions assigned to the model are:

1. Pressure far-field with the given Mac number in the  $-x$  direction

2. Pressure outlet with an atmospheric pressure of 101325 pascal.

The scheme selected in the pressure-velocity coupling is SIMPLE along with the least square Cell based gradient, second order up-wind momentum and second order pressure in the spatial discretization tab .The solution is initialized from the far field.

### 3.2 Results and discussions:

The present section deals with the study of the results obtained from the developed FE model. An aerodynamic analysis of a 2D body is performed in fluent to find out the static pressure distribution over the body. The flow conditions are taken as Mach number varying between 2 to 3 and pressure contours are plotted and compared with the benchmark paper. Energy equations are disabled while courant number is kept below 1 to prevent the solution from diverging. A converged solution of the problem is obtained after 1100 iterations. According to the results, there is a nonlinear variation in static pressure w.r.t Mac number. Pressure is maximum at Mac 2.5 and minimum at Mac 3.Further studies have proved that the static pressure increases after Mac 3.Moreover, the static pressure is maximum at the front while minimum at the sides of the body.

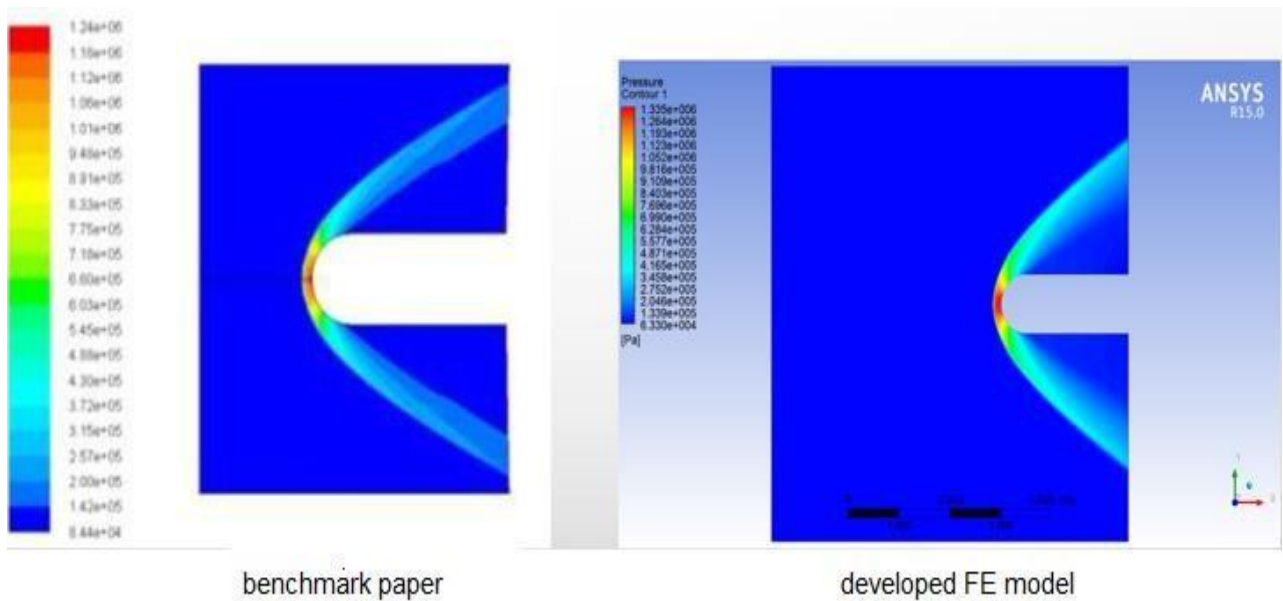


**Figure 3:**static pressure at Mac=2

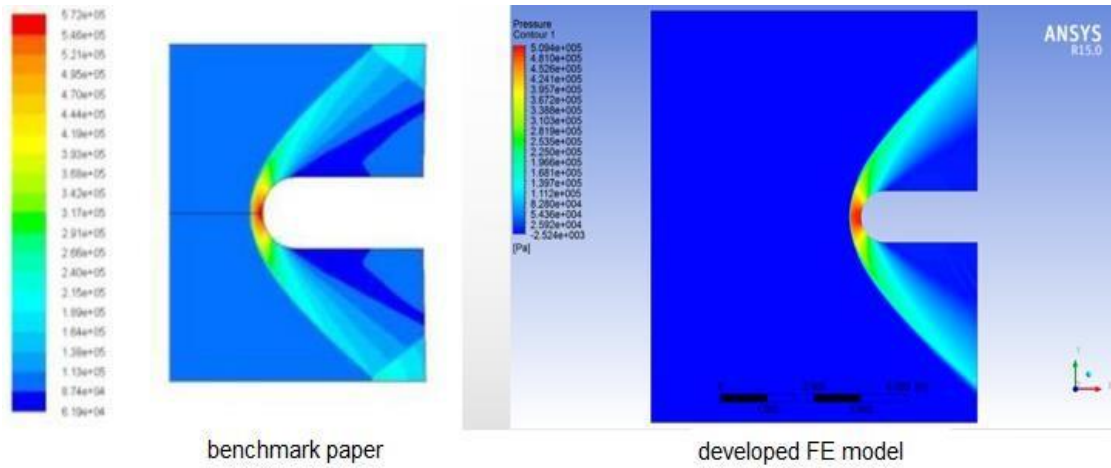


**Figure 4:**static pressure at Mac=2.5

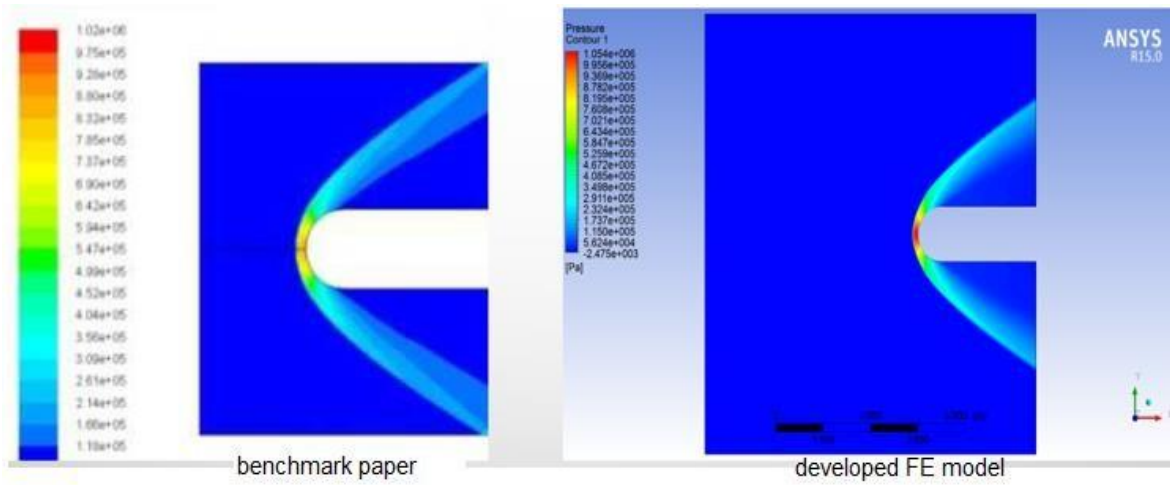


**Figure 5:**static pressure at Mac=3

### 3.3 A Summary:

A comparison of pressure contours between the developed FE model and benchmark paper at three Mac numbers is given below:

**Table 1:** A comparison

MAC	Benchmark results (static pressure )	Developed FE model (static pressure)
2	1.02 MPa	1.04 MPa
2.5	1.24 MPa	1.23 MPa
3	0.572 MPa	0.50 MPa

## **Chapter 4 Design & Development Methodology**

### **4.1 Problem Statement**

The aim of this project is to simulate a variation of temperature and pressure over a supersonic dome held in a metallic housing for a short period of time.

- 1) To find out
  1. Maximum stresses
  2. Maximum deformation
  3. Temperature difference on the outer and inner side of the dome
- 2) To study the effects of the above parameters on the
  1. Thermal shock failure
  2. Survivability of the dome
- 3) Performance evaluation of the dome for two materials-e BK7 and spinel.
- 4) To find out the most suitable material for the dome

### **4.2 Flow requirements:**

Flow requirements are important to define while designing an IR dome for supersonic flows. Two cases are solved for the dome to find out the dependency of dome failure on the flow speed. These are:

- 1) Non uniform flow from 0 to 2.5 Mac in 20 minutes for a height of 10000 ft
- 2) Non uniform flow from 0 to 3.5 Mac in 25 minutes for a height of 40000 ft



## 4.3 Ansys/Fluent

### 4.3.1 Geometric Modelling:

CAD model is divided into three regions i-e housing, adhesive and dome. These three parts are assembled to create a dome in its proper shape. In the design modular, a symmetry plane is applied to reduce the area of the model and to minimize the computational cost. Moreover, Boolean operator is utilized to subtract the geometry from the flow domain. A working domain is defined to pass the air at supersonic speed which yields the maximum temperature and pressure at the dome.

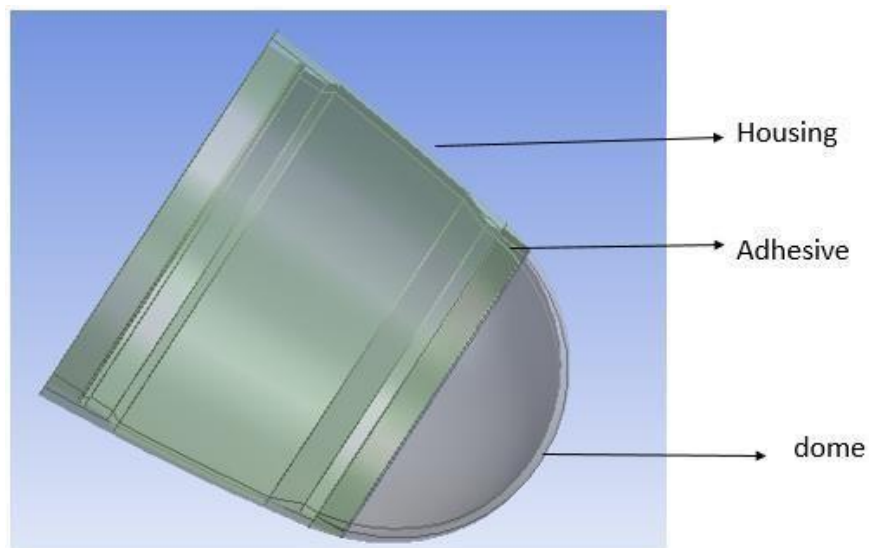


**Figure 6:**CAD model

### 4.3.2 Computational domain:

Mesh is generated using the ICEM CFD tool as shown in Figure 7 and 8 [15]. In this meshing method, the domain is finely meshed around the body. Overall, the mesh is made smooth and a density box is applied to avoid the numerical instability due to mesh problem. In addition, to capture the most important shock waves, the spacing on surface of dome is made small enough [16]. The size of domain is selected in such a way that it cannot effect the CFD results. Grid optimization was also done and an optimum mesh of 1.5 million was selected for CFD simulations.

The mesh sizes in the different regions of the model are as given below:

- ❖ Mesh size at the dome and adhesive is limited to 1.5mm.
- ❖ Mesh size at the housing is limited to 4mm.

- ❖ Prism layer method [17] is applied for 8 layers with the initial layer height of 0.0001 to keep the Y plus value below 50.
- ❖ Size of the density box is limited to 15mm with a growth ratio of 0.5.
- ❖ Mesh element size of working domain is limited to 20mm.
- ❖ Total elements :1.5 million

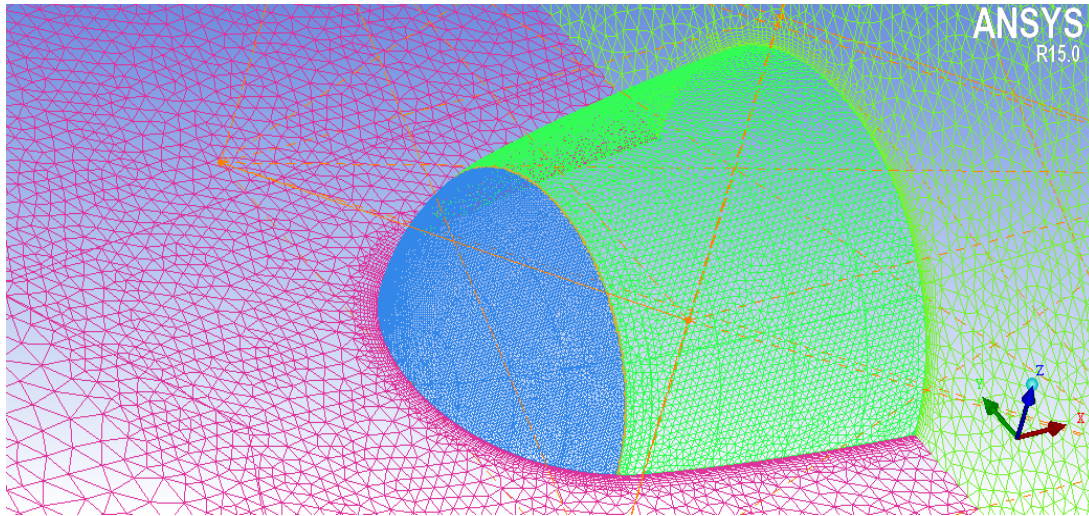


**Figure 7:**computational domain

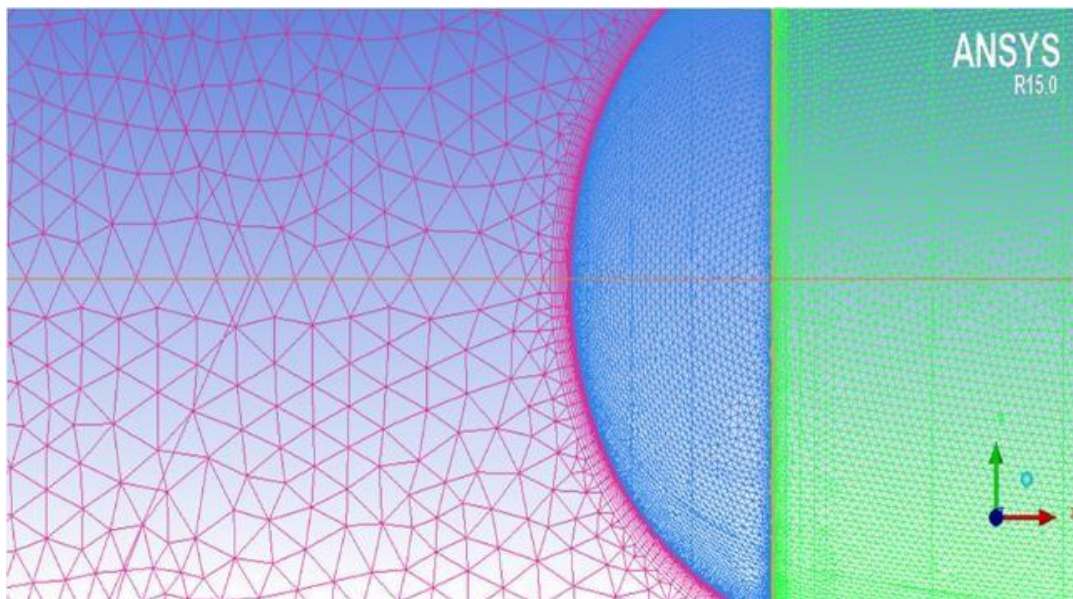


**Figure 8:**boundary layer

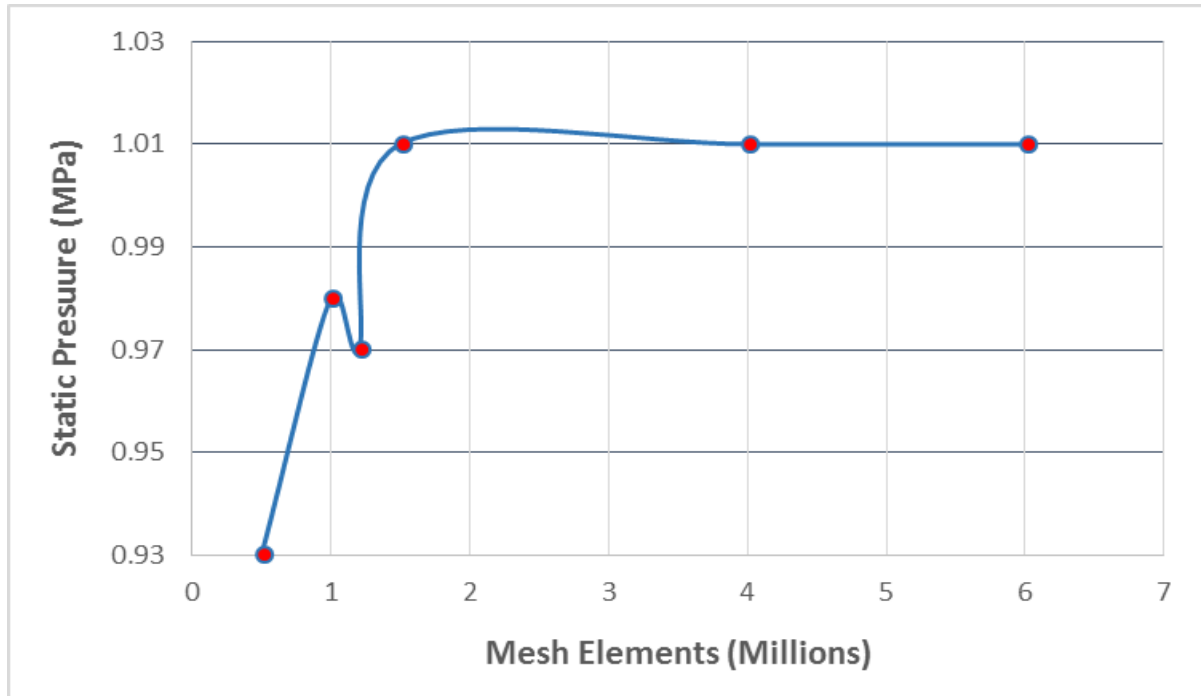
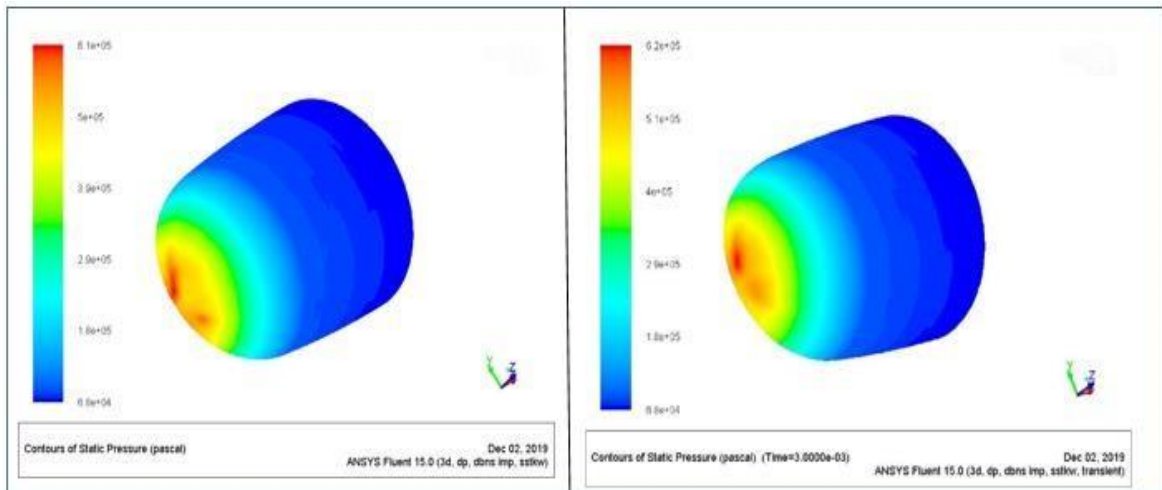


**Figure 9:Grid Independency**

### 4.3.3 Steady and transient analysis with heat transfer:

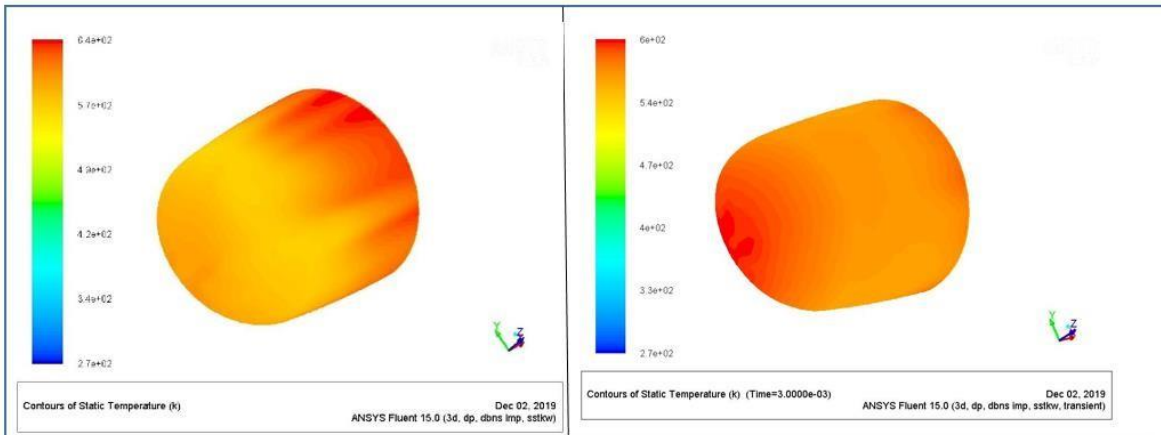
A steady and transient analysis, with heat transfer, is performed on the above defined mesh and pressure values found are verified also [18].The figures below are the results of pressure distribution over the dome flowing at Mac 4.5.



Steady case with heat transfer

Transient case with heat transfer

**Figure 10:static pressure contours at Mac=4.5**



Steady case with heat transfer

Transient case with heat transfer

**Figure 11:**static temperature at Mac=4.5

### 4.3.4 Non-uniform flow

In the next phase of the project, a non-uniform flow has been passed over a dome to find out the change in pressure and temperature over the dome w.r.t time. For instance, two cases are solved for two altitudes i-e case I for 10000ft and case II for 40000ft.A transient tabular data [19] [20]is introduced in the Fluent in which the flow is passed for 20 secs and 25 secs for case I and case II respectively. Input profiles for both the cases are given below.

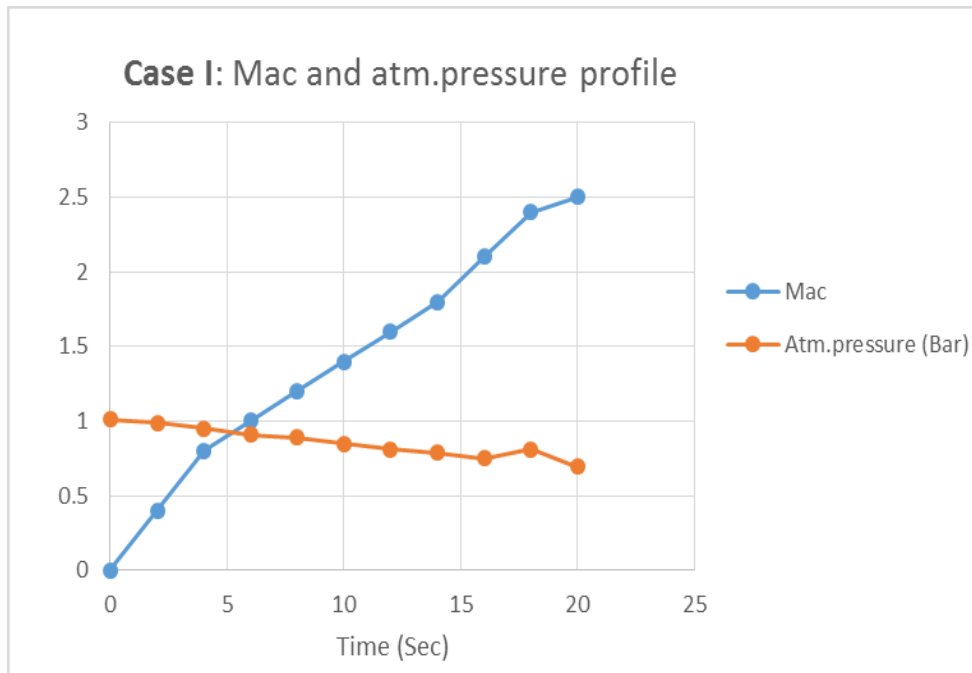


**Figure 12:**input profile for Case I

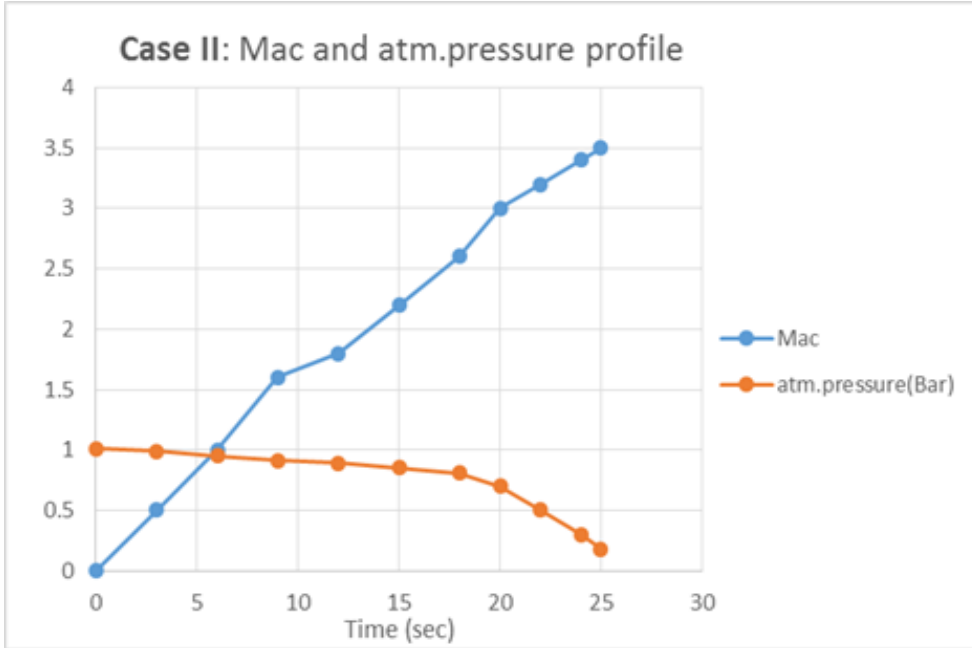


**Figure 13:**Input profile for case II

#### 4.3.5 Numerical approach:

For CFD simulations fluent software is used for flow field predictions. The Reynolds-averaged compressible Navier Stokes equations in three dimensions are solved by using finite volume spatial discretization method. For a supersonic flow, SST k-omega model is used for density based steady state flow conditions. It is a combination of world's two best models. The use of a k- $\omega$  formulation in the inner parts of the boundary layer makes the model directly usable to the wall through the viscous sub-layer and the SST formulation switches to a k- $\epsilon$  behavior in the free-stream and thereby avoids the common k- $\omega$  problem that the model is too sensitive to the inlet free-stream turbulence properties. It performs very well in adverse pressure gradient and separating flows problems.it also exhibits less sensitivity to free stream conditions and avoids a build-up of excessive turbulent kinetic energy stagnation points. CFD simulations were carried at 2.5 and 3.5 Mach & altitude of 10000 ft and 40000 ft. All the input boundary conditions in fluent are defined in the table 2.

**Table 2:**input boundary conditions

<b>Solver type /time</b>	Density based /transient
<b>Models</b>	Energy(ON) SST k-omega
<b>Materials</b>	Ideal gas; viscosity=Sutherland
<b>Cell zone condition</b>	Operating pressure=0
<b>Boundary conditions (farfield)</b>	Pressure farfield Mac=transient tabular data Pressure=transient tabular data
<b>Boundary conditions (Outlet)</b>	Pressure outlet Pressure=transient tabular data
<b>Solution method</b>	Gradient= least square Cell based Flow=first order
<b>Solution control</b>	Courant number =0.5
<b>Monitors</b>	Max Pressure and Max pressure temperature at the dome
<b>Solution initialize</b>	Standard ,farfield
<b>Run calculation</b>	Step size=0.1 Time steps=200(for case 1), 250(for case 2)



### 4.3.6 Discussion:

Density based solver is formulated for high speed compressible flows and pressure based solver is for low speed incompressible flows i-e  $Mac < 0.3$ . However, both the methods have been extended and formulated for a wide range of speeds but density based solver may give an advantage over pressure based solver for high speed compressible flows because of its accuracy. SST k omega is used for its good performance against the separating flow and pressure gradients. It models near wall interaction more accurately than k-epsilon model. Least square based cell is selected because of its accuracy in unstructured meshes and less computation cost as compare to that of node-based gradient. That is why, it is selected as a default option in ANSYS FLUENT.

### 4.3.7 Results:

The solution is run for 200 and 2500 time steps for case I and case II respectively. A time step size of 0.1 is set for both cases and 30 iterations per time step is set to converge the solution for each time step. The results obtained from fluent are plotted in figure 13 and 14. In the case I, the maximum static pressure reaches to 1MPa in the 20<sup>th</sup> second while in case II, the maximum pressure reached to 1.5 MPa in the 25<sup>th</sup> second. A same trend is followed by the temperature profile for both cases, where maximum temperature reaches to 506K and 645K for case I and case II respectively.

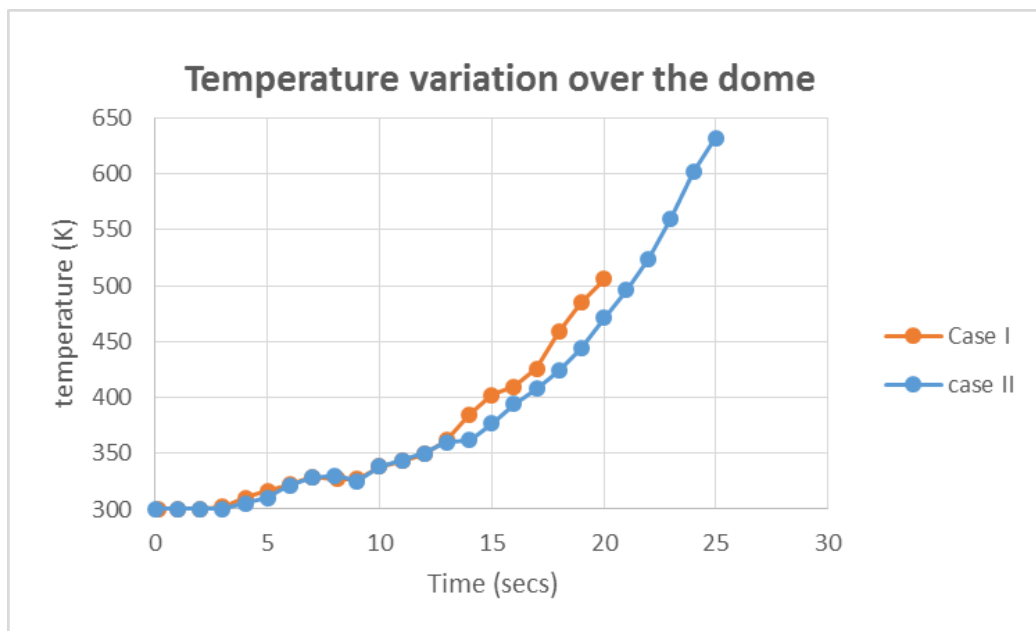


**Figure 14:**static temperature profile at the dome surface

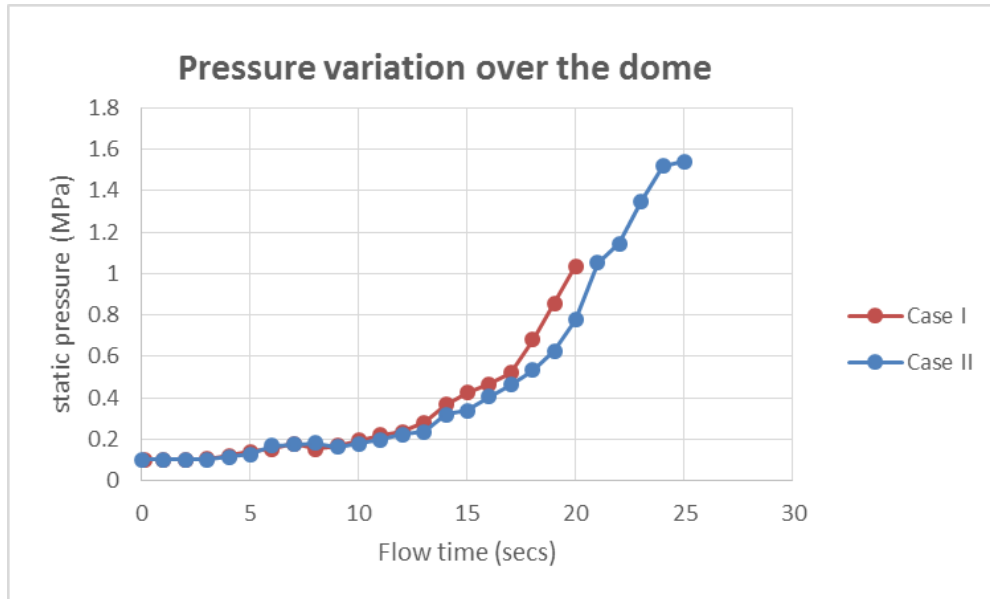


**Figure 15:**static pressure profile at the dome surface

The transient tabular data is utilized in fluent to find out the variation of pressure and temperature over a dome w.r.t time. To monitor the effects of the pressure and temperature profile over the dome, it is compulsory for a thermal-structure coupling to read the tabular data of pressure and temperature distribution over a dome which contains every time step. Moreover, fluid-structure coupling yields good results if the materials with linear properties are used only. Therefore, data from fluent is read by transient thermal analysis as a tabular data which is further coupled to transient structural analysis. Thermal-structural coupling is necessary to find out the combined effects of temperature and pressure over the body. Coupling is a computational infrastructure that allows multiple physics solvers to communicate with one another using an in-house socket-based remote procedure call library [21]

#### 4.4 Materials:

The materials selected for the dome are Bk7 and spinel while sauerisen cement and titanium alloy are assigned to adhesive and housing respectively.

Bk7 is an optical glass of high quality, performs well in all chemical test and relatively hard material with low bubbles content while providing excellent transmittance [22] [23] [24]. It is a very common crown glass used in precision lenses. On the other hand, spinel ( $MgAl_2O_4$ ) is a hard and tough crystalline material varies from colourless to red and black with excellent thermal, dielectric, optical and mechanical properties These materials makes spinel an indispensable material for domes and transparent windows. Sauereisen Cement is a chemical cement contains sodium silicate binder that



makes it ideal for ceramics, glass and other applications of high temperature [25]. Titanium alloy is assigned to housing which contains a mixture of alloy and other elements. It has very high tensile strength and toughness as well as it has the ability to withstand high temperature which is why, it is suitable for the aerodynamic applications. The properties of BK7 [26] [27] and spinel [28] are explained materials are given below

<b>BK7</b>		
<b>Density (<math>g/cm^3</math>)</b>	At 460°C	2.55
	At 510°C	2.53
	At 560°C	2.51
<b>CTE (<math>K^{-1}</math>)</b>	At 20°C	1.6E-06
	At 200°C	1.6E-05
	At 650°C	1.6E-05
<b>Young's modulus(MPa)</b>	At -100°C	82000
	At 0°C	82000
	At 100°C	81800
	At 300°C	80000
	At 400°C	78000
<b>Poison's ratio</b>	At -100°C	0.203
	At 0°C	0.203
	At 100°C	0.30
	At 300°C	0.30
	At 400°C	0.30
<b>Compressive strength (MPa)</b>		2000
<b>Tensile strength (MPa)</b>		280
<b>Thermal conductivity(<math>W/mK</math>)</b>	At 30°C	0.2
	At 100°C	0.7
	At 300°C	1.2
	At 500°C	1.23
	At 700°C	1.23
<b>Specific heat(<math>J/KgC</math>)</b>		840

**Figure 16:** properties of BK7

<b>Spinel</b>		
Density ( $g/cm^3$ )	3.58	
CTE ( $K^{-1}$ )	5.60E-06	
Young's modulus(MPa)	272500	
Poison's ratio	0.26	
Tensile yield strength (MPa)	110	
Compressive yield strength (MPa)	2690	
Thermal conductivity( $W/mK$ )	At 25°C	24.7
	At 100°C	14.8
	At 1200°C	5.4
Specific heat ( $cal\ g^{-1}\ K^{-1}$ )	0.21	

**Figure 17:**properties of spinel

## 4.5 Thermal-structural analysis:

### 4.5.1 Geometry:

The geometry for the thermal coupled analysis is the same as it was in fluent. One slight change is made in thermal analysis is that the working domain of the model is suppressed so that the pressure and temperature data can be applied on the dome.

### 4.5.2 Model and setup:

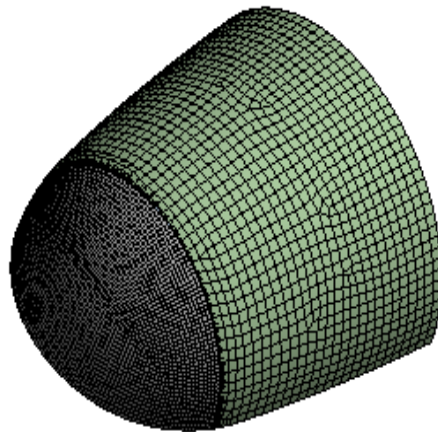


**Figure 18:**Meshing of the model

### 4.5.3 Meshing:

Meshing of the model is kept simple to avoid any uncertainty in the results. The details of meshing are:

- ❖ Method of the meshing is hexa-dominant method

- ❖ Element size of the mesh is limited to 3mm
- ❖ Element size of the mesh is limited to 5mm

#### **4.5.4 Transient thermal:**

*Case I:* As explained earlier, two cases will be solved for two altitudes. In case I Maximum mac is 2.5 which is passed over the dome in 20 seconds and it is for 10000ft altitude.

##### **Analysis settings:**

Set the step end time to 20 secs, initial subset and minimum subset to 200 and maximum subset to 2000. Insert the temperature profile as an input tabular data in the temperature bar. Run the calculation to find out the temperature difference between the outer and inner face of the dome. This difference defines the development of thermal shock in the body.

*Case II:* In case II, for a height of 40000ft, dome reaches the maximum mac of 3.5 in 25Seconds.

##### **Analysis settings:**

Set the step end time to 25 seconds. Initial subset and minimum subset to 250 and maximum subset to 2000. Insert the temperature profile as an input tabular data in the temperature bar.

#### **4.5.5 Thermal-structural coupling:**

A transient structural tab is placed on the transient thermal analysis which shares the material data, geometry and model between the two. Analysis setting remains the same between the two as explained earlier in thermal analysis. For both the cases, pressure profile is pasted in tabular form and a fixed constrain is applied to the structure for the rear side of housing. Moreover, temperature loads from the thermal analysis are imported to analyze the combine effects of temperature and pressure over the dome.

#### **4.5.6 Discussion:**

To investigate the behavior of dome at high temperature and pressure, a variable temperature and pressure curve is applied on it. Settings for Adhesive and housing remains same for both cases.

The model is fixed from the back side of housing to allow the dome to move slightly backward and fill the area where adhesive is applied. Outer surface of the dome is exposed to environment on which variable heat transfer coefficient is applied with variable ambient temperature. Thermal analysis is done on the body that will calculate all the thermal nodal values that depends on the thermal resistance of the material. A similar process takes place in structural analysis where the stresses generated due to high pressures are calculated. A thermal-structural coupling enables the workbench to display the combined effects of stresses, strain and deformation of the model [29]

**C: BK7**

Maximum Principal Stress  
Type: Maximum Principal Stress  
Unit: MPa  
Time: 20  
Custom  
Max: 87.458  
Min: -40.337  
10/14/2020 6:22 AM

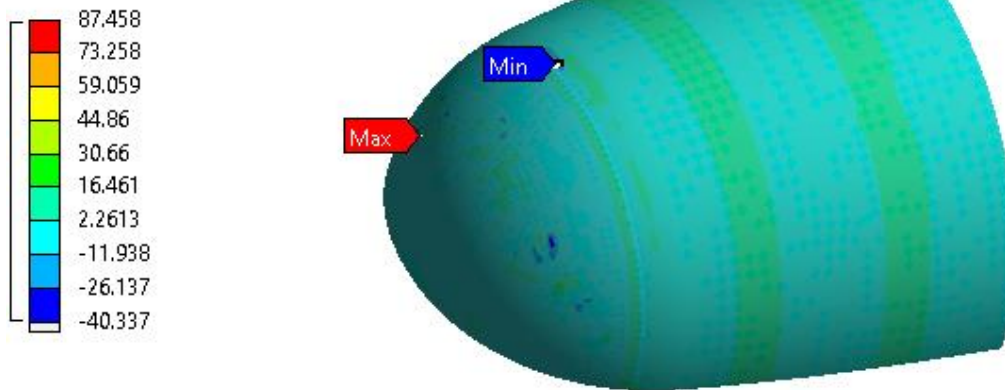


**Figure 19:**Maximum principal stresses in BK7 dome (case I)

**C: Transient Structural**

Total Deformation  
Type: Total Deformation  
Unit: mm  
Time: 20  
Max: 0.028445  
Min: 0  
4/25/2020 3:40 PM

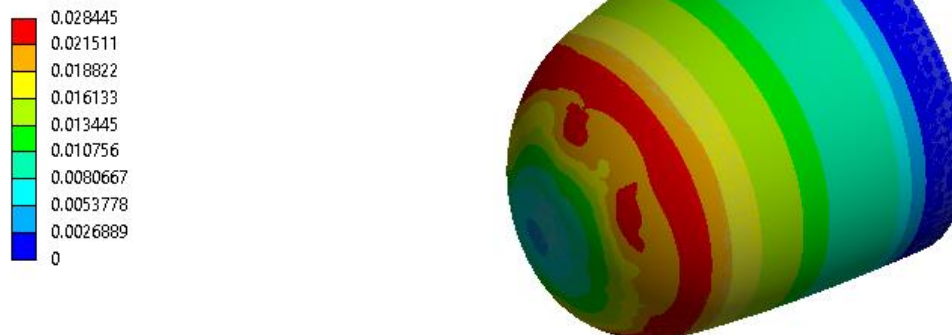


**Figure 20:**deformation in BK7 dome (case I)

**E: spinel**  
Maximum Principal Stress  
Type: Maximum Principal Stress  
Unit: MPa  
Time: 20  
10/14/2020 6:24 AM

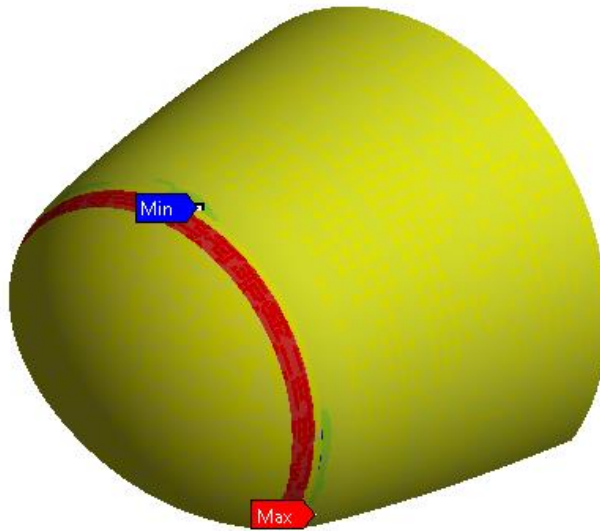
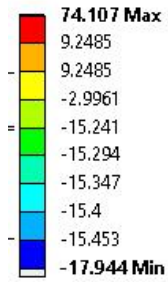


**Figure 21:** Maximum principal stress in spinel dome (case I)

**E: spinel**  
Total Deformation  
Type: Total Deformation  
Unit: mm  
Time: 20  
4/26/2020 5:51 PM

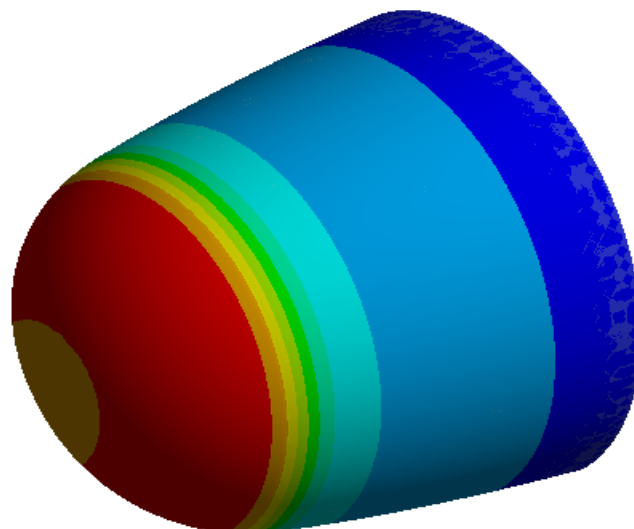
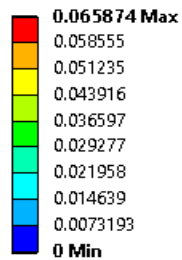


**Figure 22:** deformation at spinel dome (case I)

**D: BK7**  
Maximum Principal Stress  
Type: Maximum Principal Stress  
Unit: MPa  
Time: 25  
10/14/2020 6:27 AM

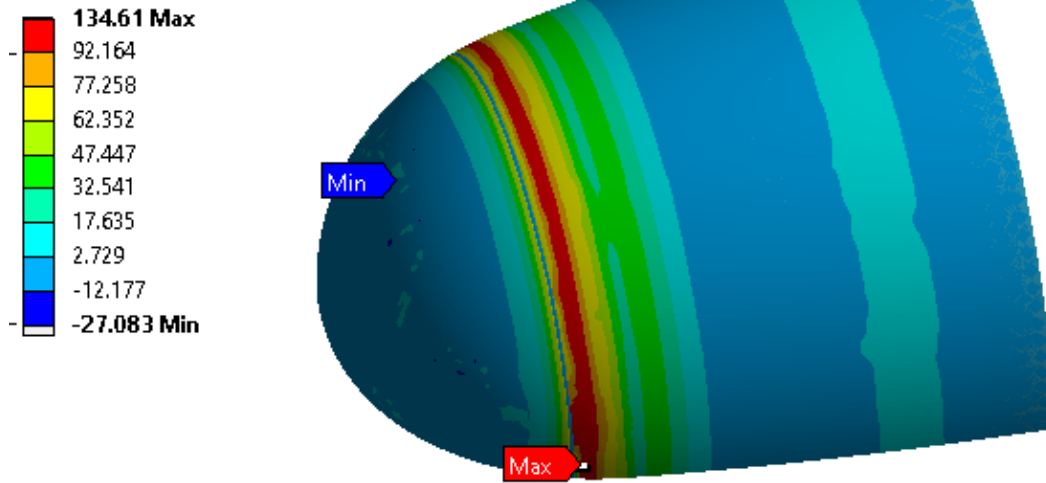


**Figure 23:**Maximum principal stresses in BK7 dome(case II)

**D: BK7**  
Total Deformation  
Type: Total Deformation  
Unit: mm  
Time: 25  
4/25/2020 3:52 PM

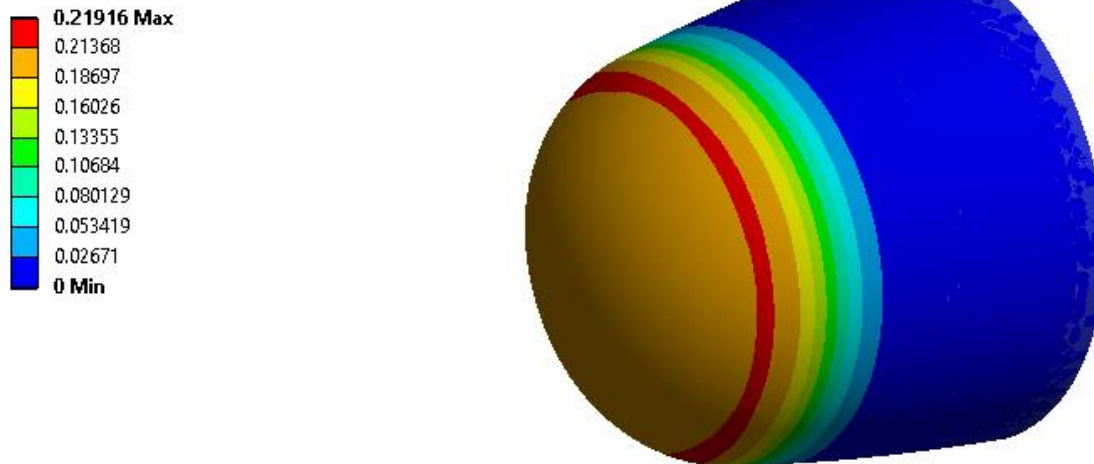


**Figure 24:**deformation in BK7 dome (case II)

**F: spinel**  
Maximum Principal Stress  
Type: Maximum Principal Stress  
Unit: MPa  
Time: 25  
Custom  
Max: 207.02  
Min: -27.398  
10/14/2020 6:30 AM

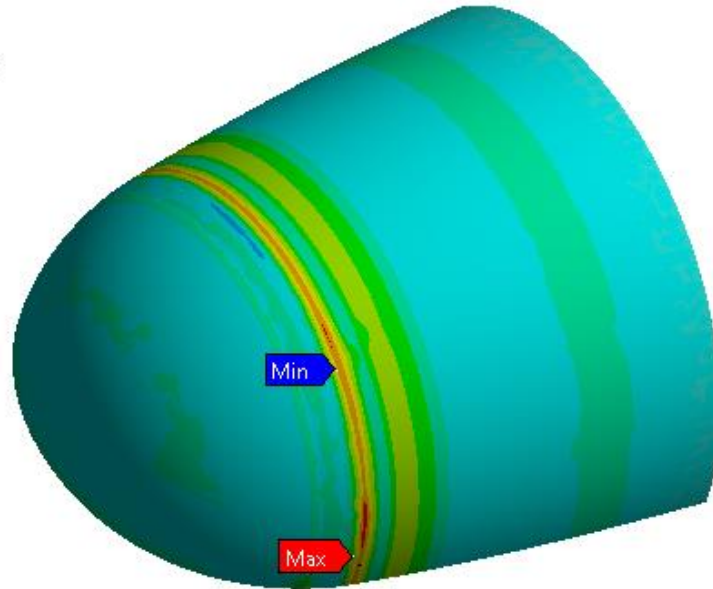
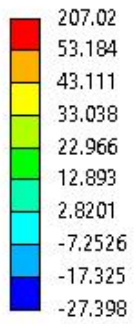


**Figure 25:**Maximum principal stresses in spinel dome (case II)

**F: spinel**  
Total Deformation  
Type: Total Deformation  
Unit: mm  
Time: 25  
4/27/2020 12:23 AM

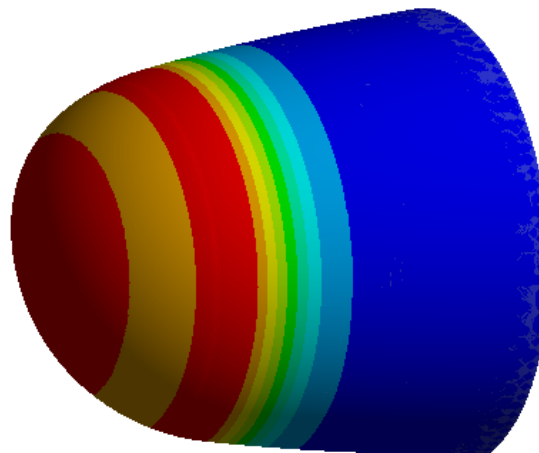
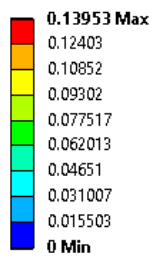


**Figure 26:**deformation in spinel dome (case II)

C: BK7  
Temperature 2  
Type: Temperature  
Unit: °C  
Time: 25  
10/9/2020 3:34 PM

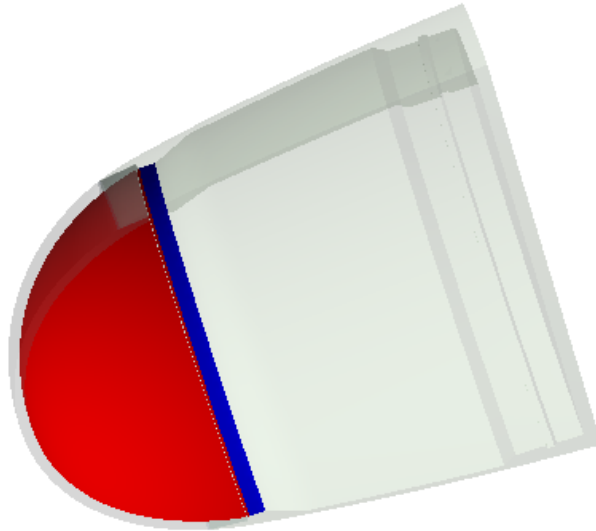
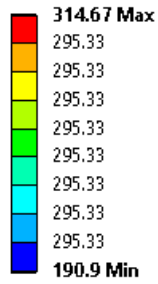


**Figure 27:** Temperature difference at the surface of BK7 dome (case I)

E: spinel  
Temperature 5  
Type: Temperature  
Unit: °C  
Time: 25  
10/9/2020 3:40 PM

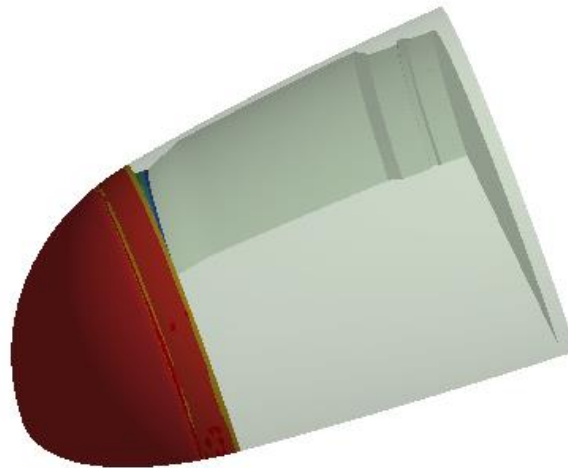
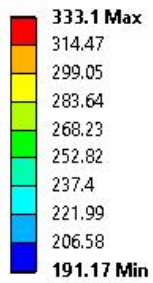


**Figure 28:** Temperature difference at the surface of the spinel dome (case I)



**Temperature 3**  
Type: Temperature  
Unit: °C  
Time: 25  
10/9/2020 3:42 PM

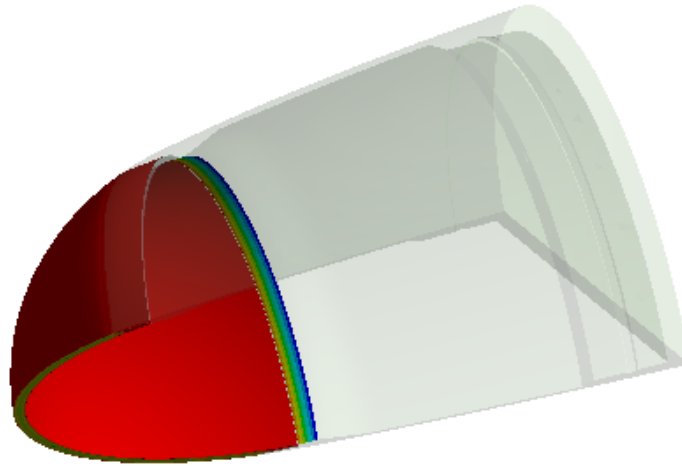
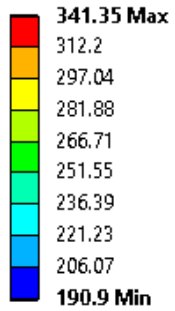


**Figure 29:**Temperature difference at the surface of the BK7 dome (case II)

**Temperature 5**  
Type: Temperature  
Unit: °C  
Time: 23.812  
10/9/2020 3:43 PM

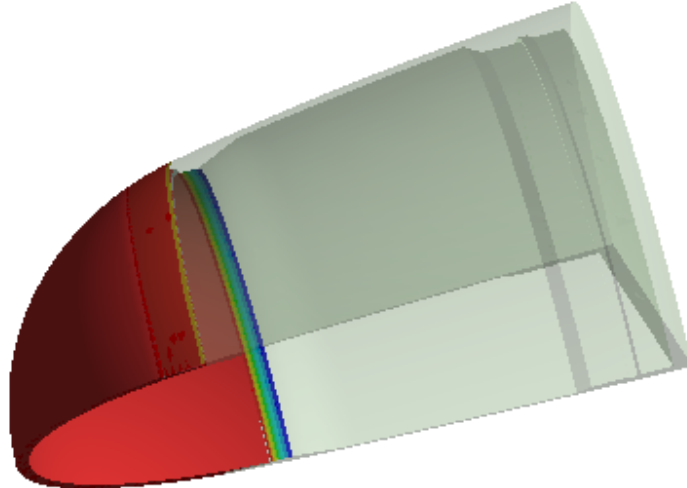
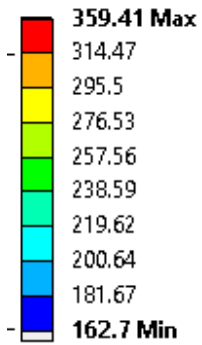


**Figure 30:**Temperature difference at the surface of the spinel dome (case II)

**B: BK7**  
Total Heat Flux  
Type: Total Heat Flux  
Unit: W/mm<sup>2</sup>  
Time: 20  
7/5/2020 1:22 AM

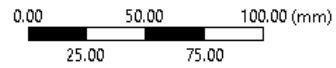
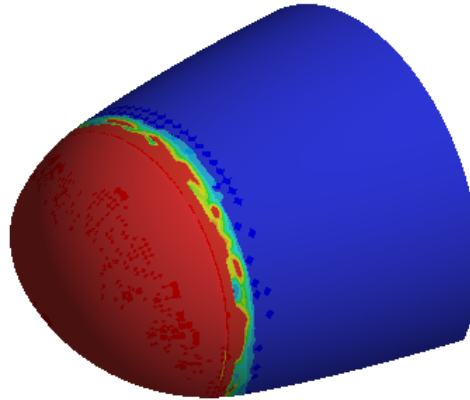
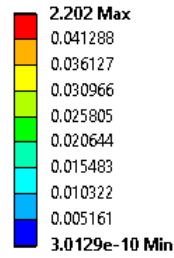


**Figure 31:**Heat flux at the BK7 dome (case I)

**D: spinel**  
Total Heat Flux  
Type: Total Heat Flux  
Unit: W/mm<sup>2</sup>  
Time: 20  
7/5/2020 1:25 AM

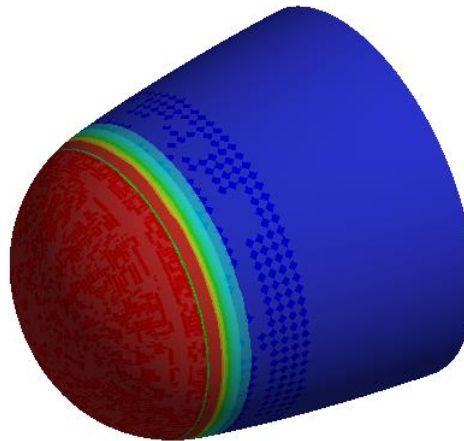
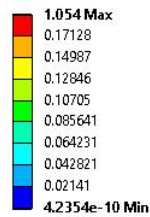


**Figure 32:**Heat flux at spinel dome (case I)

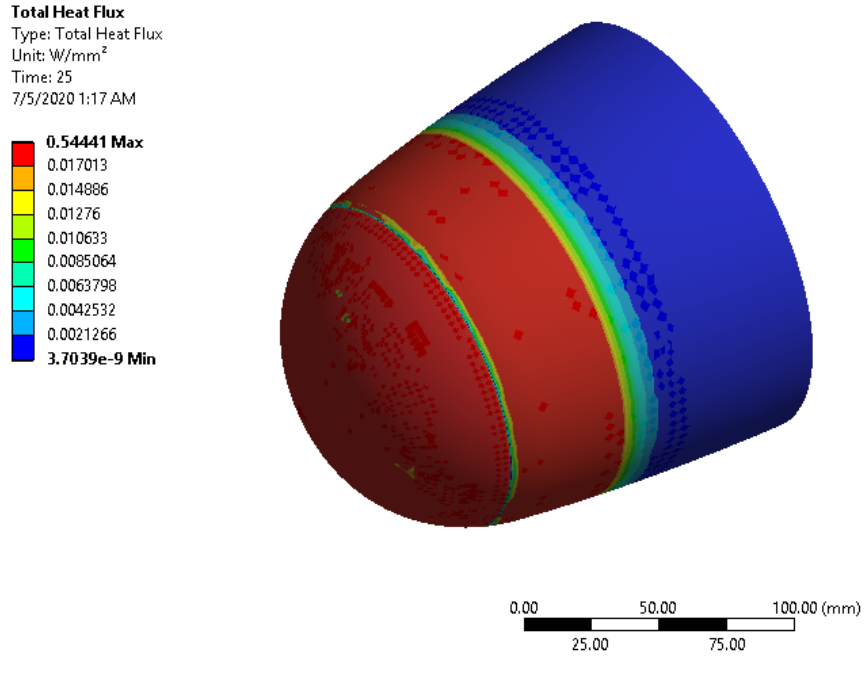


**Figure 33:Heat flux at BK7 dome (case II)**

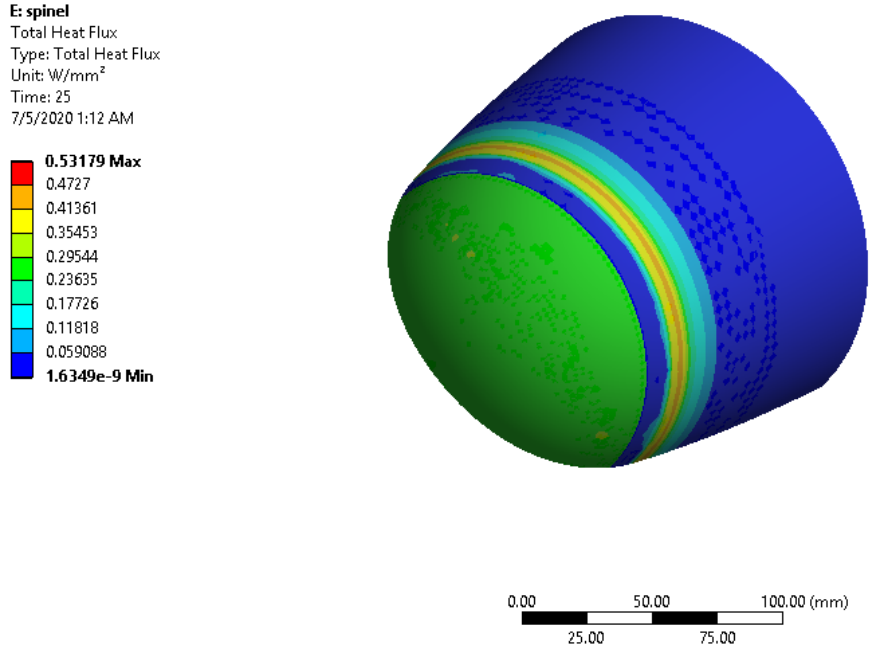


**Figure 34:Heat flux at spinel dome (case II)**

## Chapter 5 :Conclusion and future work

### 5.1 Conclusion

A sudden short period of high speed is encountered in which an IR optical dome has to bear the pressure and frictional rise in temperature. A variable flow is passed over the dome in which the pressure and temperature rises over the dome from 0 to 20 secs and from 0 to 25 secs for two cases. The maximum pressure and temperature over the dome reaches to 1.5MPa and 632K respectively in both the cases. The temporal variation of temperature and pressure over the dome is imported from fluent to transient thermal analysis and transient structural analysis respectively. Two different materials are evaluated in terms of maximum principal stress, heat flux, total deformation and temperature gradient. The properties of the materials varies with altitude and temperature. The nonlinear behavior of the materials are utilized for the thermal and structural analysis. Figure 38 and 39 shows the temporal variation of stresses over the dome.

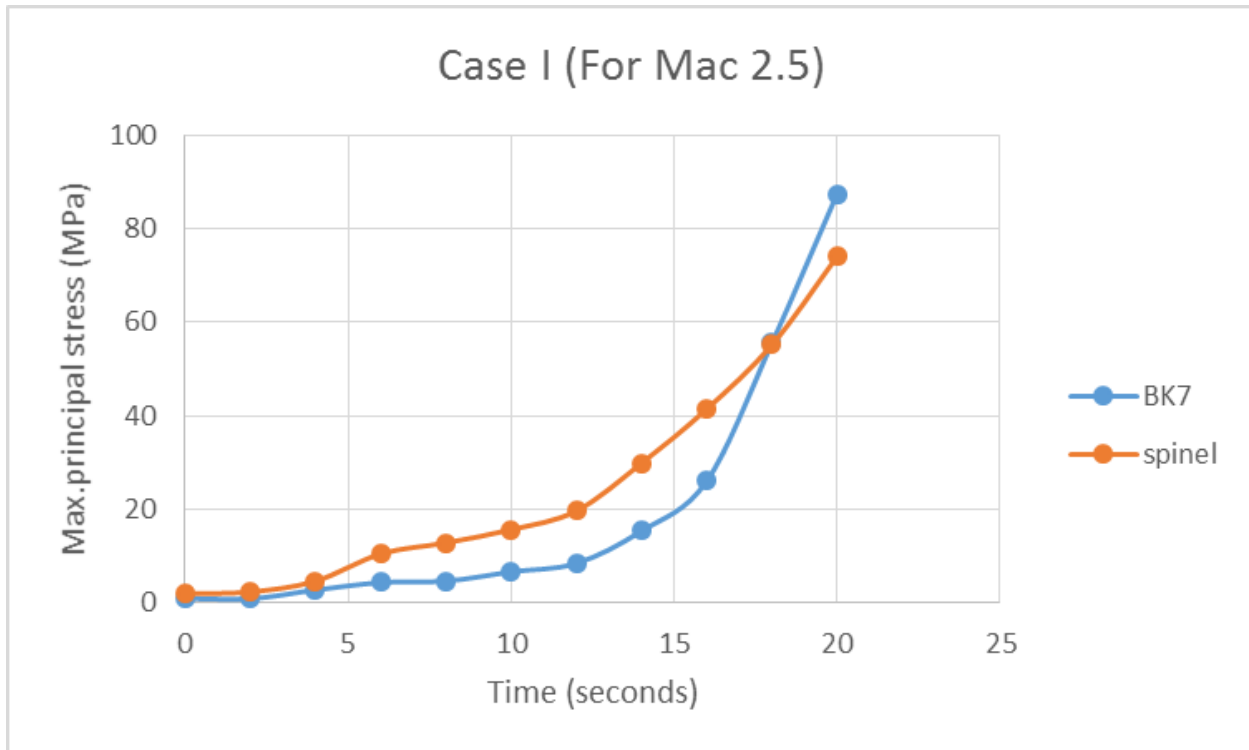


**Figure 35:**Maximum principal stresses profile for BK7 and spinel (case I)

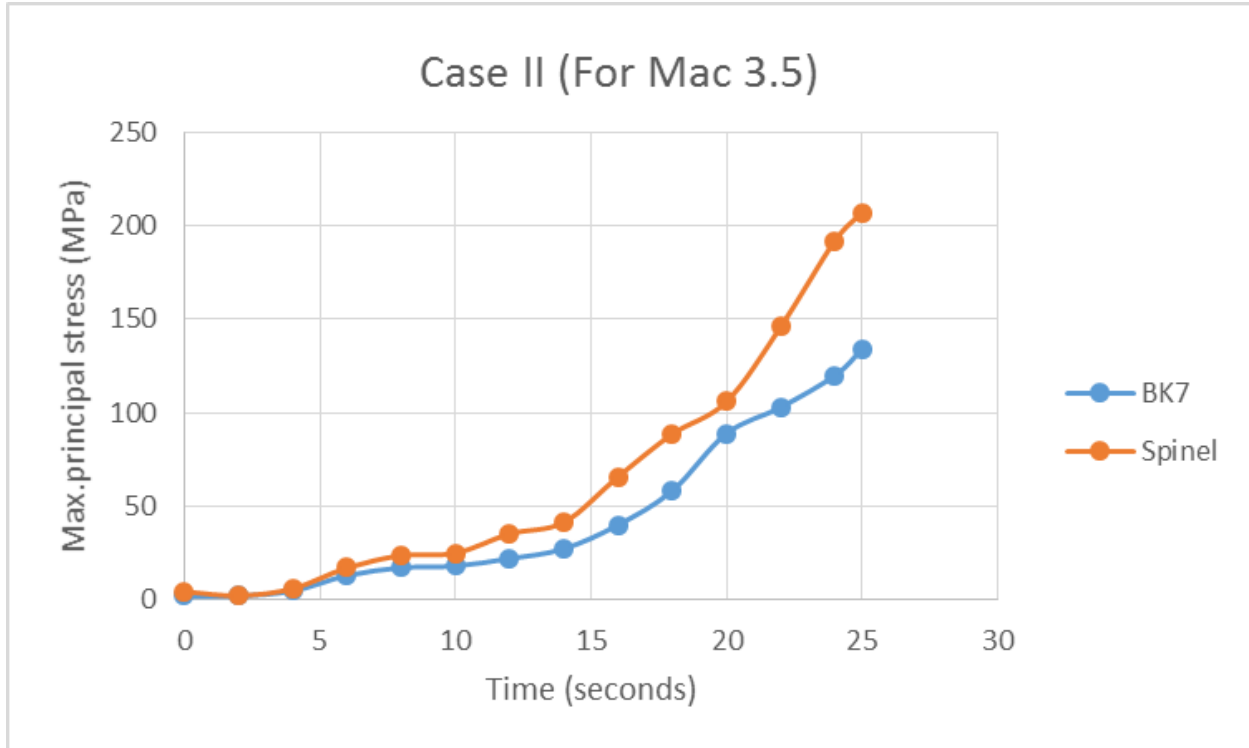


**Figure 36:**Maximum principal stresses profile for BK7 and spinel (case II)

Figures 19-30 shows the difference in the temperature between the outer and inner surface of the dome. It is clear from the figures that:

- 1) For the BK7 dome at 2.5 Mac, the difference in the temperature at surface of the dome is 124°C while the thermal shock resistance ability of BK7 is 165°C.
- 2) For the spinel dome at 2.5Mac, the difference in the temperature at surface of the dome is 142°C while the thermal shock resistance ability of spinel is 107°C.
- 3) For the BK7 dome at 3.5 Mac, the temperature difference at the surfaces of the dome is 151°C which is smaller than 165°C.
- 4) For the spinel dome at 3.5Mac, the temperature difference at surfaces of the dome is 197°C which is also greater than 107°C.

Similarly figure 35 and 36 shows that the

- 1) For BK7 glass the maximum stress generated is 134MPa
- 2) For spinel glass, the maximum stress generated is 207MPa

As both the materials used are brittle materials, Mohr-Coulomb method is applied to check the survivability of the dome. The formula for this method is

$$\text{Factor of safety (FS)} = \left( \frac{\sigma_{max}}{S_{ut}} - \frac{\sigma_{min}}{S_{uc}} \right)^{-1}$$

Where

$$\text{Safety margin} = \text{FS} - 1$$

Engineers apply both of these criteria when working on design of supersonic bodies. The result of Mohr-coulomb method are given below:

**Table 3:**Factor of Safety calculated for all the cases

MAC	Materials	
	BK7	Spinel
2.5	2.12	0.66
3.5	1.5	-0.5

It can be seen that factor of safety for spinel is less than unity.so spinel will fail in both the supersonic conditions whereas BK7 will survive.

## 5.2 Future work

This work is an offshoot of the work carried out on the different types of IR optical domes. Many tasks can be carried out on the topics related to the analysis of IR domes. As fluid analysis is important in calculating lift and drag on the body, in the future, CFD analysis could be done on IR domes. In this project, we have only gone through the mechanical properties of the dome materials but varying the dome shape for the better aerodynamic results is an area to work on. Moreover, electrical properties can also be used to find out the insertion loss, absorption loss and reflection loss. In this project, I have taken only two materials but in the future we can take different materials for multiple analysis.

## References

- [1] Y. T. Gao, "Analysis of Thermal Shock and Stress with Infrared Optical Domes," *Applied Mechanics and Materials*, pp. 332-335, 2013.
- [2] H. Qingsong Wang, "thermal shock effects on the glass thermal stress response and crack," *procedia engineering*, vol. 62, pp. 717-724, 2013.
- [3] S. hingst, "IR window design for hypersonic missiles seekers," *SPIE*, pp. 662-672, 2001.
- [4] A. X. W. Q. L. B. a. J. H. J. Zhenhai, "Thermal-structure analysis of supersonic dome based on three materials," in *International Conference on Electric Information and Control Engineering (ICEICE)*, wuhan, 2011.
- [5] F. M. D. Davis, "Design and Analysis of Different Types of radomes," *International Journal of Engineering Research & Technology (IJERT)*, 2015.
- [6] S. M. Zaharia, "CFD SIMULATION AND FEA ANALYSIS OF A BALLISTIC MISSILE," *Journal of Industrial Design and Engineering Graphics*, vol. 11, no. 2, 2016.
- [7] M. S. r. a. N. Keerthi, "Design And Structural Analysis Of Missile Nose Cone," *AUSTRALIAN JOURNAL OF BASIC AND APPLIED SCIENCES* , vol. 11, pp. 30-40, 2017.
- [8] J. H. a. G. Zeng, "Finite-element strength and stability analysis and experimental studies of a submarine-launched missile's composite dome," *engineering structures*, vol. 22, pp. 1189-1194, 2000.
- [9] Y. Y. Y. F. a. L. Z. Bin Tang, "Barium Gallogermanate Glass Ceramics for Infrared Applications," *JMST*, pp. 558-563., 2010.
- [10] T. M. H. D. F. ., W. S. Charles T. Warner, "Characterization of ALON™ Optical Ceramic," in *Proceedings of SPIE*, Bellingham, 2005.
- [11] F. S. P. H. a. P. G. J. Srulijes, "Heat Transfer at the Nose of a High-Speed Missile," *Numerical & Experimental Fluid Mechanics*, p. 373–380, 2010.
- [12] F. S. J. SRULIJES, *Analytically obtained data compared with shock tunnel heat flux measurements at a conical body at M = 6*, Berlin, Heidelberg: Springer, 2006.
- [13] C. A. Klein, "Thermal shock resistance of infrared transmitting," in *OPTICAL ENGINEERING*, 1998.
- [14] M. G. S. K. A. ., M. G. Sai Kumar A, "evaluation of effects of shapes and length of spikes on

- aerodynamics performance of supersonic Axi-symmetric bodies," *IJMOERD*, vol. 8, pp. 133-144, 2018.
- [15] N. Khan & Jameel, "numerical study of flow around a smooth circular cylinder at reynold number=3900 with LARGE eddy simulation using CFD code," in *OMAE*, busan, , 2016.
- [16] W.L.Neu, "Numerical Simulation of Flow About a Surface-Effect Ship," in *international conference on fast sea and transportation*, honolulu,hawaii,usa, 2011.
- [17] M. Lanfrit, ",Best practice guidelines for handling Automotive External Aerodynamics with FLUENT", " *Fluent Deutschland GmbH Birkenweg 14a 64295 Darmstadt/Germany*, vol. Version 1.2, 2005.
- [18] G.K.a.D.aC.math, "numerical simulation of fluid flow and aerodynamic characteristics analysis of a semi blunt 9mm bullet," *international journal of current research*, vol. 6 no.06, pp. 7278-7285, 2014.
- [19] "<https://www.afs.enea.it/project/neptunius/docs/fluent/html/ug/node225.htm>, 7.1.8 Defining Transient Cell Zone and Boundary Conditions, ANSYS.," ANSYS.
- [20] M. T. Corporation, "mide engineering solutions," 28 oct 2019. [Online]. Available: <https://www.mide.com/air-pressure-at-altitude-calculator>.
- [21] S. S. Satish Kumar Chimakurthi, "ANSYS Workbench System Coupling: a state-of-the-art computational framework for analyzing multiphysics problems," *engineering with computers*, pp. 385-411, 2017.
- [22] C. I. s. optics, "www.crystran.co.uk," oct 2014. [Online]. Available: [file:///C:/Users/shafiq%20ur%20rehman/Downloads/design-of-pressure-windows%20\(1\).pdf](file:///C:/Users/shafiq%20ur%20rehman/Downloads/design-of-pressure-windows%20(1).pdf).
- [23] D. L. & Y. H. & Y. Tang, "Relationship between subsurface damage and surface," *Int J Adv Manuf Technol*, p. 613–622, 2013.
- [24] W. G. a. Z. Yao, "Evaluation of surface cracking in micron and sub-micron scale scratch tests for optical glass BK7," *Journal of Mechanical Science and Technology* 25, p. 1167~1174, 2011.
- [25] s. c. no.32, "www.environmental expeert.com," july 2019. [Online]. Available: <https://d3pcsg2wj9izr.cloudfront.net/files/1703/download/832549/21-32-potting-cement.pdf>.
- [26] A. O. S. AG, "Mechanical and thermal properties of optical glass," SCHOTT AG, Hattenbergstrasse 10 55122 Mainz Germany, 2018.
- [27] makeitfrom, "makeitfrom.com," [Online]. Available: <https://www.makeitfrom.com/material-properties/Borosilicate-Glass>. [Accessed 20 march 2020].
- [28] Ganesh, "A review on magnesium aluminate (MgAl<sub>2</sub>O<sub>4</sub>) spinel: synthesis, processing and



- applications," *International Materials Reviews*, pp. 63-112, 2013.
- [29] A. A. Sweta Jain, "Coupled Thermal – Structural Finite Element Analysis for Exhaust Manifold of an Off-road Vehicle Diesel Engine," *International Journal of Soft Computing and Engineering*, vol. 3, no. 4, 2013.
- [30] J. Zhenhai, A. Xingqiao, W. Qun, L. Bo and J. Hongguang, "Thermal-structure analysis of supersonic dome based on three materials," in , *International Conference on Electric Information and Control Engineering (ICEICE)*, Wuhan, China, 2011.
- [31] F. M. Denish Davis, "Design and Analysis of Different Types of," *International Journal of Engineering Research & Technology (IJERT)*, 2015.
- [32] W. S. M. D. Luca Mangani, "Comparing the performance and accuracy of a pressure based and a density-based coupled solver," in *HAL* , USA, 2018.